

# An Engineered Biomaterial Microenvironment to Direct the Formation of a Living Barrier to Seal Cartilage Defects

Jay M Patel, PhD<sup>1,2</sup>  
 Claudia Loebel, MD, PhD<sup>2,3</sup>  
 Brian C Wise, BS<sup>1,3</sup>  
 Kamiel S Saleh, BS<sup>1,2</sup>  
 James L Carey, MD, MPH<sup>1</sup>  
 Jason A Burdick, PhD<sup>3</sup>  
 Robert L Mauck, PhD<sup>1,2,3</sup>

<sup>1</sup> McKay Orthopaedic Research Laboratory  
 University of Pennsylvania

<sup>2</sup> Translational Musculoskeletal Research  
 Laboratory  
 Corporal Michael J Crescenzo VA Medical  
 Center

<sup>3</sup> Department of Bioengineering  
 University of Pennsylvania

## Introduction

Articular cartilage consists of a dense extracellular matrix that allows the tissue to undergo fluid pressurization during compressive loading. Cartilage defects compromise this function, introducing free boundaries that result in the flow of proteoglycans and other matrix elements out of the tissue.<sup>1</sup> Decreases in matrix density at defect boundaries make them vulnerable to progressive erosion, instigating a vicious cycle that gradually increases defect size and concludes with joint-wide osteoarthritis (OA). A barrier at this interface may functionally restore the mechanical properties of the defect boundary<sup>2</sup>, however synthetic materials may wear or delaminate with time. In this study, we aimed to direct the formation a living fibrous barrier at the damaged cartilage interface (via targeted progenitor cell recruitment and differentiation—Figure 1A), to restore normal cartilage biomechanical function. Specifically, we sought to establish a biomaterial microenvironment (modified hyaluronic acid) that 1) enhances the attachment and mechano-biological response of MSCs at the damaged cartilage interface, 2) induces the cells to undergo fibrogenesis via mechanical cues, and 3) promotes the deposition of fibrous matrix.

## Methods

### Biomaterial Microenvironment

Methacrylated hyaluronic acid (MeHA; 75kDa, 35-42% modification) was conjugated with fluorescent peptides (FITC) for visualization and fibronectin-mimicking peptides (RGD) for cellular adhesion (Figure 1B). The material was oxidized to introduce aldehydes (~30% substitution), which form covalent linkages with exposed amines in damaged tissue.<sup>3</sup>

### Cellular Response

Bovine cartilage plugs were retrieved and sectioned (6mm diameter × 100µm thick). These discs were maintained as naïve samples (ND; mimicking a focal defect) or were digested in collagenase (0.01% for 30 minutes) to mimic degenerated cartilage (D). Biomaterial was applied with 0, 5 or 15 minutes of UV cross-linking, followed by PBS washes to remove non-adhered biomaterial. Cartilage discs (both ND and D) without biomaterial served as controls. Disc-biomaterial composites were seeded with juvenile bovine MSCs (P1-P3, 500 cells per disc) for 24 hours. Samples were fixed in 10% buffered formalin, followed by staining for F-actin with phalloidin to quantify cellular spread area and

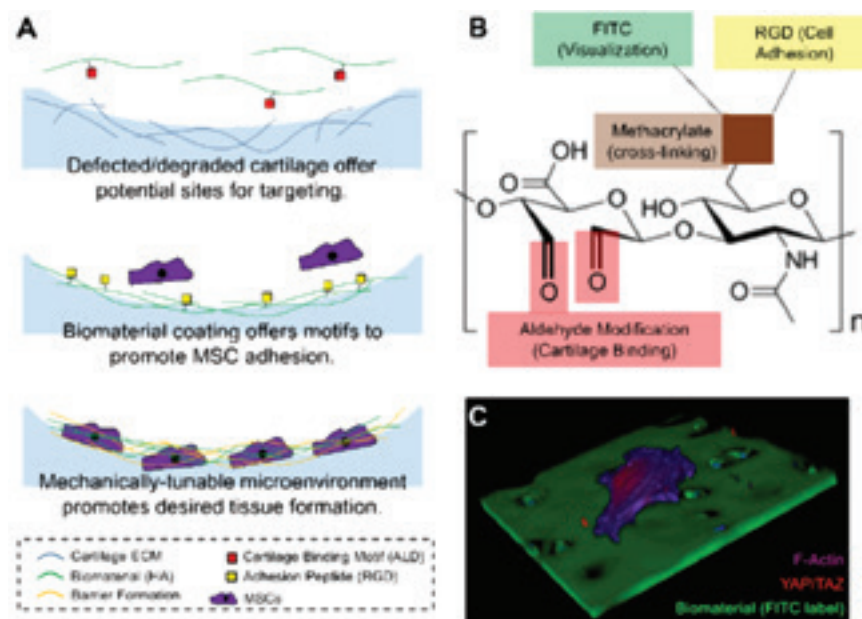


**Figure 1.** Approach Schematic. **(A)** Schematic of biomaterial binding to damaged cartilage, promoting MSC adhesion, and ultimately guiding cells towards formation of a barrier; **(B)** Biomaterial design with modifications to hyaluronic acid (HA); **(C)** Example of material applied to cartilage disc, with an adhered MSC.

for the nuclear co-factors YAP/TAZ to quantify cell mechano-response (Figure 1C).<sup>4</sup> YAP/TAZ signal intensity in the nucleus and cytoplasm were quantified to obtain a measure of nuclear localization (> 100 cells per group).

### Fibrogenesis and Matrix Deposition

Additional cartilage discs (both ND and D) were subjected to biomaterial application/cross-linking. Discs were seeded with 500 cells and cultured for seven days in basal media. Cells on the discs were fixed and stained for  $\alpha$ -smooth muscle actin ( $\alpha$ -SMA), a marker of fibrogenesis.<sup>5</sup> The percentage of cells positive for  $\alpha$ -SMA fibers was calculated for six replicates. Finally, an additional set of samples (ND vs D, no biomaterial vs biomaterial + 15 min UV) were cultured in medium containing L-azidohomoalanine (AHA), an alternative to L-methionine that incorporates into newly-deposited matrix. Subsequently the AHA can be stained with fluorescently-labeled dibenzocyclooctyne (DBCO) in order to visualize matrix deposition.

### Statistical Analysis

Cell area and YAP/TAZ nuclear ratio were analyzed with a one-way analysis of variance (ANOVA) with post-hoc Tukey's test.  $\alpha$ -SMA data was compared using a replicate-matched Kruskal-Wallis test. ND and D samples were analyzed separately.

## Results

Confocal microscopy showed that the MeHA biomaterial infiltrated throughout the 100 $\mu$ m section prior to cross-linking, forming an integrated biomaterial microenvironment, around and in between chondrocytes in the cartilage matrix (Figure 1C). The biomaterial also promoted MSC adhesion (Figure 1C, Figure 2A) to the tissue-biomaterial interface, increasing cell spread area (Figure 2B). Biomaterial application and cross-linking increased YAP/TAZ nuclear localization (Figure 2C) of MSCs on both non-degraded and degraded cartilage, consistent with the increased MSC spread area (Figure 2B) and higher substrate mechanical properties (Figure 2A—insets) with biomaterial augmentation.

MSCs cultured for 7d on both nondigested and digested cartilage discs (without biomaterial; Figure 3A top) yielded a low percentage of cells positive for  $\alpha$ -SMA fibers (13.96 and 6.95%, respectively). Biomaterial application/cross-linking (Figure 3A, bottom) significantly increased (Figure 3B) the percent of  $\alpha$ -SMA positive MSCs on both nondigested and digested discs, indicating enhanced fibrogenesis.

Finally, samples without biomaterial (ND, D) showed little to no matrix deposition, as visualized by AHA staining (Figure 4, top). Conversely, application of biomaterial prior to cell seeding promoted new matrix formation (Figure 4, bottom).

## Discussion

The results of this study detail the use of a modified biomaterial to 1) promote attachment and mechano-sensation of MSCs; 2) guide attached cells towards a fibrogenic

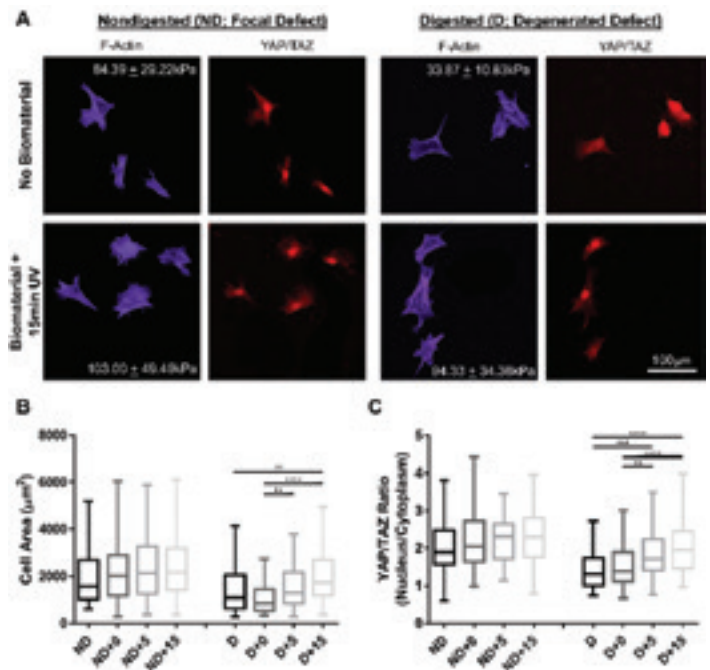


**Figure 2.** Cell Spreading and YAP/TAZ. (A) Representative images of F-actin and YAP/TAZ in cells on nondegraded and degraded samples, both without biomaterial (top row) and with biomaterial and cross-linking (bottom row); Quantification of (B) cell spread area and (C) YAP/TAZ ratio (nuclear:cytoplasmic) of cells on ND and D samples without biomaterial, with biomaterial (+0), and with biomaterial and crosslinking (+5, +15).  $n > 100$  cells per group. \*, \*\*, \*\*\*, \*\*\*\* indicate  $p < 0.05, 0.01, 0.001, 0.0001$ , respectively.

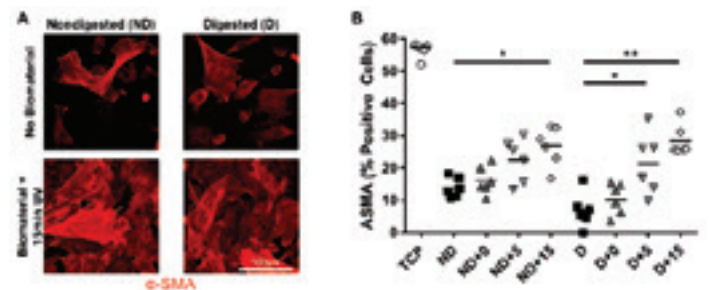


**Figure 3.**  $\alpha$ -Smooth Muscle Actin. (A) Representative images of cells stained for  $\alpha$ -SMA; (B) Percentage of cells positive for  $\alpha$ -SMA stress fibers.  $n > 50$  cells per data point ( $n = 6$  replicates). \*, \*\* indicate  $p < 0.05, 0.01$ , respectively.

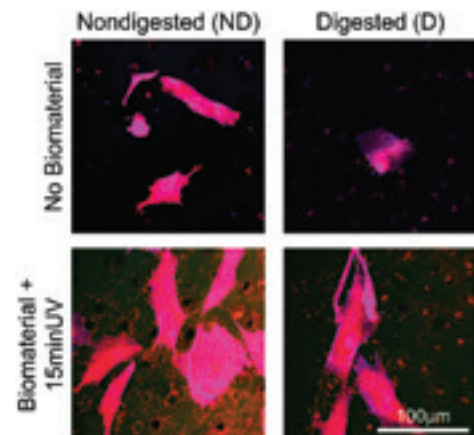


**Figure 4.** Matrix Deposition. Red stain depicts incorporation of AHA into new matrix. Biomaterial application and crosslinking results in increased deposition (bottom row). Scale bar depicts 100 microns.

phenotype; and 3) promote matrix deposition to cover cartilage defects. These findings support the promise of creating tunable microenvironments to home and retain stem cells at the defect interface, and ultimately control their biologic response. The behavior of cells in this study is consistent with prior cell-hydrogel studies, in that cell attachment and fibrogenesis increase with substrate stiffness. The biomaterial microenvironment in this study does just that, as it utilizes both cell-adhesive and mechanical cues at the damaged interface to induce a fibrotic response. Future studies will investigate the ability of the tissue barrier to functionally seal defects and preserve cartilage integrity in both *in vitro* cartilage explant and *in vivo* trochlear defect models.

## Acknowledgements

This work was supported by the NIH, VA, AOSSM, and CEMB. The authors thank the Mauck and Burdick Labs at Penn for their help.

## References

1. Basalo IM, Mauck RL, Kelly TN, *et al.* Cartilage interstitial fluid load support in unconfined compression following enzymatic digestion. *J Biomech Eng* 2004; 126(6): 779-786.
2. Grenier S, Donnelly PE, Gitten J, *et al.* Resurfacing damaged articular cartilage to restore compressive properties. *J Biomech* 2015; 48(1): 122-129.
3. Wang DA, Varghese S, Sharma B, *et al.* Multifunctional chondroitin sulphate for cartilage tissue-biomaterial integration. *Nat Mater* 2007; 6(5): 385-392.
4. Dupont S, Morsut L, Aragona M, *et al.* Role of YAP/TAZ in mechanotransduction. *Nature* 2011; 474(7350): 179-183.
5. Talele NP, Fradette J, Davies JE, *et al.* Expression of alpha-smooth muscle actin determines the fate of mesenchymal stromal cell. *Stem Cell Rep* 2015; 4(6): 1016-1030.